CrossMark

ORIGINAL PAPER

# A model of stem growth and wood formation in *Pinus radiata*

**David M. Drew**[1] · **Geoff Downes**[2]

## Abstract

***Key message*** **A model of wood formation processes in pines predicted 80 % of mean wood density variation from inputs of carbohydrate allocation and tree water status from several varied sites.**

*Abstract* Numerous factors determine how wood properties vary as a tree grows. In order to model wood formation, a framework that considers the various xylogenetic processes is required. We describe a new model of xylem development and wood formation in pines (parameterised for the commercially important species, *Pinus radiata* D. Don). In this paper, we use as inputs simulated daily data from the CaBala stand growth model which, in turn, takes into account site and daily weather conditions, and silviculture. It incorporates a first attempt at predicting microfibril angle (the angle of cellulose microfibrils relative to the vertical axis of the cell, MFA) based on metrics of cambial vigour and carbohydrate allocation. It also predicts tracheid dimensions and wall thickness, and from these data, wood density. Pith-to-bark and intra-annual variation in predicted wood properties was realistic across a wide range of site types, although juvenile wood properties were weakly predicted. The model was able to explain 50 % of the variation in outerwood MFA and 70–80 % of the variation in outerwood and mean sample wood density respectively, from 17 study sites. The model, early results from which are very promising, provides a useful framework for testing concepts of how formation occurs, and to provide insights into areas where further research is needed.

**Keywords** Cambium · Pinus radiata · Secondary thickening · Carbohydrate allocation · Wood density · Microfibril angle · Xylem

## Introduction

Wood is one of the most abundant and vital resources in the world, representing a renewable source of energy, fibre and construction material (Zhang et al. 2014). Laid down continuously in perennial plants, the formation of wood occurs as a series of inter-related processes, beginning with the division of cells in a narrow meristem called the cambium and ending with the formation of empty conduits with thickened, lignified walls (Philipson et al. 1971). The collective processes of xylem differentiation are generally referred to as "xylogenesis" (Wardrop 1981). Over recent decades a growing body of research has accumulated concerned with the question of xylogenesis, particularly focussed on a range of molecular biochemical and biophysical aspects of the process (see for example Fromm 2013; Harashima and Schnittger 2010; Li et al. 2012; Oda and Fukuda 2012; Zhang et al. 2014). It is important to incorporate these new insights into predictive models that capture aspects of xylem formation to better explain wood property variation in trees growing under a wide range of conditions.

Many of the physical properties of xylem tissue (e.g. wood density) are a function of varying durations and rates of cellular enlargement and secondary wall thickening

✉ Geoff Downes
geoff.downes@forestquality.com

1   CSIRO Sustainable Agriculture Flagship, Private Bag 12, Hobart, TAS 7001, Australia

2   Forest Quality Pty. Ltd., P.O. Box 293, Huonville, TAS 7109, Australia

(Fritts 1976). Much research has been directed at quantifying and understanding variation in xylem developmental dynamics, in softwoods (e.g. Denne 1971, 1976; Horacek et al. 1999; Lupi et al. 2014; Rossi et al. 2006b, 2008; Skene 1969, 1972) and hardwoods (e.g. Catesson and Roland 1981; Drew and Pammenter 2007; Lachaud 1989; Ridoutt and Sands 1994). This has informed the development of a range of models designed to simulate cambial activity and ultimately wood property variation (Deckmyn et al. 2006; Deleuze and Houllier 1998; Drew et al. 2010; Fritts et al. 1999; Hölttä et al. 2010; Kramer 2002; Meicenheimer and Larson 1983; Vaganov et al. 2006; Wilson 1964; Wilson and Howard 1968). Nevertheless, there is much about wood formation that is not understood, with room for improvement in our models.

In a commercial context, faster growth rates achieved by improvements in breeding and silviculture have frequently resulted in harvestable volumes at younger ages, but often with negative wood quality implications (Apiolaza et al. 2013; O'Hehir and Nambiar 2010). To deal with this, there is an increasing shift in the management and breeding of commercial species like *Pinus radiata* D. Don towards wood quality improvement (Wu et al. 2008) and the focus of research into wood quality variation needs to deal with the nexus between site, silviculture, genetics and the value of products (Downes and Drew 2008). In landscapes where growing conditions are highly variable, the interactions of site, genotype, management and climate, particularly over time, are beyond the scope of easily implemented empirical approaches. In this paper we describe a new model of wood formation processes in pines, applicable across broad regional landscapes. While focused on *P. radiata* D. Don, a species of major commercial importance globally (Gavran and Parsons 2011), we believe the model could be applicable to softwoods generally.

The model takes a simple approach to handling cambial division, tracheid growth and wall thickening, relying mainly on a small set of readily available/simulated variables, with fluctuating tree water status and carbohydrate balance being of primary importance as drivers. We hypothesized that this approach would be sufficient to explain variation in within-tree (pith-to-bark patterns) and site mean wood density, as well as tracheid dimensions in plantation-grown *P. radiata* across a range of growing conditions. Further, we hypothesized that this could be achieved with a single set of constraining parameters, making the model relatively generic.

## Materials and methods

### Model development approach

The model we report here based on existing concepts of wood formation in the literature, as well as on insights gained into short-term growth responses and wood formation dynamics from ongoing research. It represents in some regards an advancement/adaptation of an earlier framework developed for *Eucalyptus* spp (Drew et al. 2010), although it introduces a completely new approach to some elements of modelling xylem differentiation.

### Study sites

For the development and testing of the model in the form presented in this paper, we used data from 17 sites at which *P. radiata* had been established commercially, or in research trials (Table 1). We defined 21 site × management × climate regimes (hereafter termed "scenarios") for analysis, as at some sites trees were managed in multiple ways. That is, although trees were at the same "site", they were treated as separate study cases.

Six of the sites were established as "model development" sites at which detailed measurements of tree stem growth were made using automated electronic point dendrometers. Measurements of radial change in stem size (over-bark) were made hourly. In conjunction with detailed growth measurements, cambial micro-core samples were taken from three sites on four separate occasions in 2010 and 2011 using a Trephor corer (Rossi et al. 2006a), and immediately placed in FAA fixative solution (35 % distilled water/50 % ethyl alcohol/% glacial acetic acid/10 % formaldehyde). Samples were later reduced in size, mounted in resin, and sectioned to 4 μm. These sections were mounted on slides, and viewed using a Zeiss Axioscope microscope (Zeiss, Oberkochen, Germany). The numbers of cells in the dividing (cambial) zone and subsequent stage of permanent enlargement were counted, based on increasing radial diameter and the onset of secondary thickening (determined by detecting birefringence in the cell wall). Wood core samples were then taken at the end of monitoring, and pith to bark variation in wood density, tracheid diameter, wall thickness and microfibril angle (MFA) was measured at 0.025–0.1 mm resolution on 6–12 samples per site using the CSIRO SilviScan system (Evans 1994; Evans and Ilic 2001).

At all other sites, DBH was measured only periodically or at the time of wood sampling, but pith-to-bark variation wood density and MFA was measured in detail using SilviScan, and information was also available on the the relationship between wood property data and sawn board characteristics. These latter sites were selected as having low, moderate and high average outer-wood density (based on 50 mm increment cores) taken at breast height and thus represented much of the variation in the regional resources from which they were sampled.

### Model runs

The model uses as inputs stand-level simulations of forest growth and canopy processes. In this paper, we used input

**Table 1** Sites used for model development and testing

| Scenario | Latitude (South) | Site silviculture summary | Basic soil description | MAT (°C)/MAP (mm) |
|---|---|---|---|---|
| Balmoral | 42.00 | Planted 1997 at 833 SPH | Silt loam over clay | 11.6/610 |
| | | Dendrometers installed 2008 | | |
| Blackwarry (Strzelecki ranges) | 38.40 | Planted 1995 at 1111 stems/ Ha | Clay loam over saprolith | 10.9/1300 |
| | | Thinned 2010 to 595 stems/ Ha | | |
| | | Dendrometers installed 2010 | | |
| Byjuke | 37.50 | Planted 1975 at 1600 stems/ Ha | Sand | 14.0/640 |
| | | Thinned 1985 to 720 stems/ Ha | | |
| | | Thinned 1989 to 550 stems/ Ha | | |
| | | Thinned 1996 to 250 stems/ Ha | | |
| Caroline HQ | 37.90 | Planted 1958 at 1736 stems/ Ha | Loamy sand | 13.8/775 |
| | | Thinned 1970 to 1070 stems/ Ha | | |
| | | Thinned 1981 to 750 stems/ Ha | | |
| | | Thinned 1988 to 450 stems/ Ha | | |
| | | Thinned 1994 to 250 stems/ Ha | | |
| Emerson's | 38.00 | Planted 1976 at 1736 stems/ Ha | Clay loam | 13.7/830 |
| | | Thinned 1983 to 600 stems/ Ha | | |
| | | Thinned 1996 to 340 stems/ Ha | | |
| Flynn (2 regimes modelled) | 38.25 | Planted 1995 at 1111 stems/ Ha | Sandy loam over clay | 14.0/800 |
| | | Planted 1995 at 1111 stems/ Ha | | |
| | | Thinned 2008 to 200 stems/ Ha | | |
| | | Dendrometers installed 2011 | | |
| Kentbruck | 38.05 | Planted 1970 at 2000 stems/ Ha | Loamy sand | 13.9/840 |
| | | Thinned 1985 to 750 stems/ Ha | | |
| | | Thinned 1993 to 388 stems/ Ha | | |
| | | Thinned 1999 to 250 stems/ Ha | | |
| Kongorong | 37.90 | Planted 1974 at 2000 stems/ Ha | Clay loam | 14.0/760 |
| | | Thinned 1980 to 630 stems/ Ha | | |
| | | Thinned 1988 to 443 stems/ Ha | | |
| | | Thinned 2000 to 273 stems/ Ha | | |
| Long's | 37.70 | Planted 1965 at 1379 stems/ Ha | Loamy sand | 13.5/840 |
| | | Thinned 1977 to 590 stems/ Ha | | |
| | | Thinned 1983 to 495 stems/ Ha | | |
| | | Thinned 1992 to 250 stems/ Ha | | |

**Table 1** continued

| Scenario | Latitude (South) | Site silviculture summary | Basic soil description | MAT (°C)/MAP (mm) |
|---|---|---|---|---|
| Longford | 38.4 | Planted 1972 at 1667 stems/ Ha | Sand | 11.0/1345 |
| | | Thinned 1984 to 1000 stems/ Ha | | |
| | | Thinned 1991 to 560 stems/ Ha | | |
| McGillivray's | 37.80 | Planted 1970 at 1600 stems/ Ha | Sand | 14.0/675 |
| | | Thinned 1982 to 830 stems/ Ha | | |
| | | Thinned 1988 to 440 stems/ Ha | | |
| | | Thinned 1995 to 270 stems/ Ha | | |
| Mt Gambier airport (3 regimes modelled) | 37.75 | Planted 1995 at 2268 stems/ Ha | Sand | 13.7/720 |
| | | Thinned 2000 to 1111 stems/ Ha | | |
| | | Thinned 2007 to 555 stems/ Ha | | |
| | | Planted 1995 at 1111 stems/ Ha | | |
| | | Thinned 2007 to 555 stems/ Ha | | |
| | | Planted 1995 at 555 stems/Ha | | |
| | | Dendrometers installed 2010 | | |
| Myora | 37.85 | Planted 1969 at 1905 stems/ Ha | Loamy sand | 13.9/780 |
| | | Thinned 1981 to 750 stems/ Ha | | |
| | | Thinned 1987 to 450 stems/ Ha | | |
| | | Thinned 1994 to 220 stems/ Ha | | |
| Nangeela | 37.50 | Planted 1977 at 1401 stems/ Ha | Sand | 13.8/650 |
| | | Thinned 1988 to 807 stems/ Ha | | |
| | | Thinned 1999 to 375 stems/ Ha | | |
| Ohurakura | 40.00 | Planted 1993 at 625 SPH | Sand | 12.0/1840 |
| | | Dendrometers installed 2008 | | |
| Porter's road | 38.90 | Planted 1979 at 1736 stems/ Ha | Clay loam | 13.8/870 |
| | | Thinned 1997 to 642 stems/ Ha | | |
| | | Thinned 2002 to 362 stems/ Ha | | |
| Reedy Creek | 36.25 | Planted 1996 at 1600 stems/ Ha | Sand over clay with water table present | 14.0/500 |
| | | Thinned 2005 to 760 stems/ Ha | | |
| | | Thinned 2010 to 520 stems/ Ha | | |
| | | Dendrometers installed 2011 | | |

from the CaBala model (Battaglia et al. 2004), which provides detailed daily outputs of the variables required by our cambial model: daily minimum and maximum leaf water potential, carbohydrate allocated to stem, stand density, tree height and crown length. Cabala runs on a daily time-step, using daily minimum and maximum temperature, relative humidity, rainfall and incoming solar radiation as key inputs, as well as detailed soil descriptions.

It utilises a sophisticated approach to dealing with site variability, incorporating models of soil water availability and nitrogen mineralisation. Furthermore, Cabala incorporates complex silvicultural simulation elements, taking into account the effects of different types or levels of forest thinning, pruning and fertilisation on tree physiological processes. A set of species- or germplasm-specific parameters limits model simulations for a particular scenario.

A single parameter set previously developed for *P. radiata* (unpublished data, courtesy of Ms. Jody Bruce and Dr. Michael Battaglia) was used for all runs. The predictions were tested against pith-to-bark radial profiles of wood density and MFA data from all study sites and tracheid radial diameter and wall thickness data from a subset of 6 sites (for which it was available).

# Model development and description

## Model organisation

At the onset of a simulation, an initial set of hypothetical cells is created and assigned meristematic status. Thereafter, for each daily time step, stand-level data are re-calculated to a tree level (see below) or to the level of a particular height up the stem (e.g. breast height) for which the simulation is being run. That is, all relevant environmental variables, as expressed in the CaBala outputs which are fed into the cambial model, that contribute to xylem developmental processes are calculated for each day *d*. Once the tree- and stem position-level variables have been calculated, the program considers each cell in the growing hypothetical population and performs the following operations for day on cell *c*:

1. The allocation of daily carbohydrate to each living xylem cell.
2. The determination of cell developmental stage.
3. The determination of cell division (only for meristematic cells).
4. Cell enlargement.
5. Cell secondary thickening and microfibril angle.
6. Cell death.

The effects of the varying environmental conditions on cell growth and differentiation for each day and cell *c* (if applicable) are described according to the equations presented below.

## Parameters

To bound predictions in the cambial model, 22 parameters must be defined for a 'genotype' (Table 2). Values listed in Table 2 represent a functional set indicative of what

would broadly be expected of *P. radiata* across a range of sites. They should not necessarily be considered as final or complete, and indeed, further parameterization is ongoing.

## Tree-level variables

Calculations of variables are first made at an individual tree level (conceptually, the "average" tree in the stand). As a result, input stand level data must first be converted to the appropriate unit. Most critically, the daily NPP (i.e. total sequestered carbohydrate minus respiratory demand) allocated to the stem for the individual "average" tree $X$ (kg) on day is calculated (Eq. 1).

$$\text{NPP}_{\text{stem}_t} = \left( \left( \text{NPP}_{\text{stand}} / \text{SPH} \right) \times 1000 \right) \times \text{alloc}_{\text{stem}} \qquad (1)$$

where $\text{NPP}_{\text{stand}}$ is the NPP for the stand (t/ha), SPH is the stand density (trees/ha) and $\text{alloc}_{\text{stem}}$ is the allocation to stem (%) on day.

Cambial surface area on day is calculated using a 3-dimensionally parabolic representation of stem shape. This calculation requires the diameter of the tree at the base. For this reason, the model needs to run at two positions in parallel: the position of interest to the user (e.g. breast height), and at the base of the tree (nominally 5 cm above ground level) for a basal diameter estimate. An area specific available carbohydrate (ASC) value $(\text{g}/\mu\text{m}^2)$ is then calculated for tree $X$ on day (Eq. 2).

$$\text{ASC}_{\text{stem}} = \left( \text{NPP}_{\text{stem}_t} \times 1000 \right) / \left( \text{SA}_{\text{stem}} \times 10^{12} \right) \qquad (2)$$

where $\text{NPP}_{\text{stem}_t}$ is defined in Eq. 1, and $\text{SA}_{\text{stem}}$ is the surface area of the stem (underbark) $(\text{m}^2)$ on day.

## Carbohydrate allocation

To simulate xylem development at any height up the stem, a number of position-level variables are calculated at each time step. First, the total carbohydrate available for the modeled developing cell file $f$ (g) is calculated (Eq. 3):

$$\text{Carbs}_f = \left( \text{ASC}_{\text{stem}} + \text{Stored Carbs}_f \right) \times \text{Tan Area}_{\text{tracheid}}$$
$$(3)$$

where $\text{ASC}_{\text{stem}}$ is defined in Eq. 2, Stored Carbs$_f$ is the amount of non-structural carbohydrates (calculated as the daily sum of "left over" carbohydrates not used on day-1) in addition to new allocation available for the modeled cell file $f$ (g) on day, and Tan Area$_{\text{tracheid}}$ is the area of the tangential face of the average tracheid in the cell file $(\mu\text{m}^2)$ on day.

Each day a critical osmotic potential $(\Psi_{\pi_{\text{crit}}})$ (MPa), is calculated (Eq. 4), below which the model tries to maintain the average osmotic potential of the dividing and enlarging

**Table 2** Parameter symbols, descriptions and values used in the analysis described in this paper

| Parameter symbol used in the text | Parameter description and units | Estimate parameter value | Source/s |
|---|---|---|---|
| $\gamma_{SUC_{CD}}$ | The critical concentration of carbohydrates for the cessation of secondary thickening (g/ml) | 0.1 | Estimated from sucrose concentrations measured in xylem sap during the growing season (Sauter 1980, 2000) |
| $\alpha_L$ | The proportion of cell length after a cell division | 0.9 | Estimated |
| $\alpha_{EZ/CZ_{max}}$ | The target ratio of enlarging to cambial cells (# EZ cells/# CZ cells) | 0.7 | Measured and see Barnett (1973) |
| $\theta_{max}$ | Maximum wall extensibility (μm/MPa/day) | 16 | Estimated |
| $MFA_{max}$ | The maximum angle of microfibrils in the $S_2$ wall layer (degrees) | 70 | Barnett and Bonham (2004) and measured |
| $L_{max}$ | The maximum length of a mature tracheid (μm) | 3000 | Skene (1969) |
| $\emptyset_{max}$ | The maximum diameter of a mature tracheid (μm) | 56 | Measured |
| $\alpha_{wall_{max}}$ | The maximum ratio of wall area to cell cross sectional area (μm$^2$/μm$^2$) | 0.86 | See Skene (1969) and measured |
| $\Delta V_{wall_{max}}$ | The maximum rate of wall thickening (μm$^3$/day) | 20,000 | Calculated from data presented in Skene (1972) and Dodd and Fox (1990) |
| $f_{MFA}$ | Factor determining MFA responsiveness to carbohydrate allocation across the differentiating zones | 0.4 | Optimised |
| $t_{div_{min}}$ | The minimum time required between successive cell divisions (cell cycle) (day) | 3 | See Skene (1969) |
| $\emptyset_{div_{min}}$ | Minimum radial diameter for periclinal division (μm) | 12 | Measured and see Barnett (1973) |
| $\Psi_{\pi_{min}}$ | The minimum osmotic potential achievable by differentiating cells in the cambial zone (MPa) | −2.6 | Based on estimates in leaves from Woodruff et al. (2004) and unpublished glasshouse data (pers. comm. Dr. P. Mitchell) |
| $T_{min}$ | The average daily air temperature at which metabolic activity in the developing xylem is inhibited [deg C] | 4 | Estimated from temperatures limiting to growth suggested in Feikema et al. (2010) |
| $\Psi_{p_{crit}}$ | The target turgor for growing cells (MPa) | 1 | See Steppe and Lemeur (2007) |
| $\propto_{\Delta\emptyset L}$ | Ratio of tracheid length/radial growth (μm/μm) | 10 | Estimated |
| $f_{vac}$ | Scaling factor to adjust from lumen volume to the "effective" volume for osmotic adjustment | 0.055 | Optimised |
| $\rho_{CW}$ | Density of the cell wall (g/cm$^3$) | 1.5 | Kellogg and Wangaard (1969) |
| $\Psi_{p_{YT}}$ | The cell wall yield threshold (MPa) | 0.3 | See Steppe and Lemeur (2007) and Meinzer et al. (2008) |
| $f_{juv}$ | Distance from crown apex at which juvenile production completely ceases (m) | 8 | Estimated based on an 8–10 ring "juvenile core" and assuming height growth ∼1 m/year |
| $\partial c_{max}$ | The rate at which carbohydrate is transferred directly across the secondary thickening zone during latewood formation (μm/day) | 2 | Estimated |
| $\emptyset_{TTD}$ | Tracheid tangential diameter (μm) | 30 | Measured |

cells in the modeled cell file (for turgor maintenance). This depends largely on the water potential in the xylem and the availability of carbohydrates to drive osmotic potential (Duan et al. 2013; Hölttä et al. 2010). It is anticipated that xylem growth occurs predominantly at night when water potentials are recovering (Downes et al. 1999, 2004; Zweifel et al. 2005, 2007), and therefore only pre-dawn xylem water potential (a measure of effective maximum water availability at the site) is considered. Average turgor potential in the growing and dividing cell populations is maintained above or at a target turgor potential (a parameter, $\Psi_{p_{crit}}$, in MPa) to prevent desiccation damage, and under suitable circumstances, facilitate growth. Target turgor is modified at positions less than $f_{juv}$ (a parameter, in m) from the top of the tree, to a minimum of $0.9 \times \Psi_{p_{crit}}$. To protect the cambium against very cold temperatures, $\Psi_{\pi_{crit}}$ is also modified as a function of cold temperature (coming into effect only below the minimum temperature for cambial activity ($T_{min}$), with the effect reaching a maximum at −5 °C).

$$\Psi_{\pi_{\text{crit}}} = \min \begin{cases} \Psi_{x_{\max}} - \Psi_{p_{\text{crit}}} \\ (T_{\min} - (-5))\big/(T_{\text{crit}} - (-5)) \times \Psi_{\pi_{\min}} \end{cases} \tag{4}$$

where $\Psi_{x_{\max}}$ is maximum xylem water potential (an input from CaBala) on day and $\Psi_{p_{\text{crit}}}$, $T_{\min}$, and $\Psi_{\pi_{\min}}$ are parameters. The base temperature below which cells are fully protected against frost damage is set at $-5$ °C.

The model then optimizes cambial width and the width of the enlargement zone by trying to ensure that the average osmotic potential of cells in those zones is equal to or slightly below $\Psi_{\pi_{\text{crit}}}$.

### Annual seasonality

Consideration of seasonality is an important part of the allocation procedure. Although *P. radiata* can produce multiple branch whorls per year, and is highly responsive to suitable growth conditions (Fernández et al. 2011), it still produces a clear, annual growth ring in most circumstances (Walcroft et al. 1997). That is, even if it produces false rings, an annual ring will still generally form (even at sites which are not very cold). The model, induces latewood development seasonally, triggered using day length (Fromm 2013). A number of studies have shown that, in various conifers, the timing of maximum growth rates occur around the summer solstice, followed by a decreasing growth rate thereafter (Duchesne et al. 2012; Rossi et al. 2006c) and the almost immediate onset of latewood characteristics in cells (Vavrčík et al. 2013). The same has been observed in radiata pine [e.g. Boardman 1988 and in dendrometer data from our study (data not shown)].

Changes in growth, however, are the culmination of multiple morphological and phenological changes in the tree that also occur seasonally, such as induction of reproductive buds or cone production and associated changes in hormone balances or other mechanisms of developmental control (Fernández et al. 2011; Fromm 2013; Paulina Fernández et al. 2007; Savidge and Wareing 1981). It has been shown, for example, that photosynthetic capacity at the leaf level peaks in many temperate species at the summer solstice(Bauerle et al. 2012) and Gricar et al. (2007) showed that prior to the summer solstice, local cambium heating and cooling had an effect, whereas afterwards they did not, probably because of hormonal control. At various times, such as the summer solstice, the developing zone of xylem in all likelihood enters an altered physiological state, with changes potentially including a changed allocation priority associated with maximum summer drought.

During earlywood formation, allocation to dividing and enlarging cells is prioritised. The main period of earlywood formation is defined in the model to occur while day length is increasing (provided other factors are not limiting), or while day length is decreasing but still less than 99 % of the longest day at the site. Thereafter, the priority of direct allocation to cells in which secondary thickening is underway is increased. That is, for each day after latewood has begun, the width of the secondary zone to which carbohydrate is directly transferred is increased by an amount $\partial c_{\max}$ (a parameter, µg/day).

In the model carbohydrate concentrations decrease in cells further from the phloem (Uggla et al. 2001). Carbohydrate will be allocated to a cell, provided the osmotic potential of cell $c$ in the cell file is above the minimum value possible ($\Psi_{\pi_{\min}}$). An allocation coefficient ($\alpha_{\text{alloc}}$) is calculated for each day using an optimization routine to ensure that the allocation across the zone of cells to which carbohydrate is allocated exceeds 99 % of the total available allocation (Alloc$_f$) for the whole cell file $f$, on day. The allocation of carbohydrate to any cell $c$ (g) is then calculated as described in Eq. 5.

$$\text{Alloc}_c = (\text{Alloc}_f - \text{Alloc}_{c-1}) \times \alpha_{\text{alloc}} \tag{5}$$

where Alloc$_f$ is the amount of carbohydrate available for allocation to the entire cell file $f$ (g), Alloc$_{c-1}$ is the allocation previously committed to the cell one position closer to the phloem than cell $c$ (g) and $\alpha_{\text{alloc}}$ (defined above) is the allocation coefficient for day.

For each cell, a cumulative carbohydrate quantity is monitored. This total carbohydrate content is used to calculate the osmotic potential of the cell $c$ on day (Eq. 6).

$$\Psi_{\pi_c} = \varphi \times -1 \big(\gamma_{\text{SUC}_e} \times R \times T\big)\big/1000 \tag{6}$$

where $\varphi$ is the osmotic coefficient of sucrose ($\sim 1.4$), $\gamma_{\text{SUC}_e}$ is the effective concentration of sucrose (mol/L) (see Eq. 7), $R$ is the gas constant (0.0821) and $T$ is the average temperature (K) on day.

$$\gamma_{\text{SUC}_e} = \text{Suc}\big/(\text{Vol}_{\text{lum}} \times f_{\text{vac}}) \tag{7}$$

where Suc is the quantity of sucrose in solution in the osmotically active volume of the cell (mol), Vol$_{\text{lum}}$ is the lumen volume (L) on day and $f_{\text{vac}}$ is a parameter scaling to the effective volume.

### Stages of tracheid development and differentiation

Unlike hardwoods, softwoods produce one main longitudinal cell type in the xylem (Haygreen and Bowyer 1982). Therefore all cells on the pith-side of the cambium are considered merely as "xylem", and only xylem cells are followed through all stages of differentiation. Cells that exit to become phloem cells are immediately removed from the population and not considered further (to reduce run time), although with some

**Fig. 1** The relationship between the number of cambial initials and enlarging cells in the same cell file
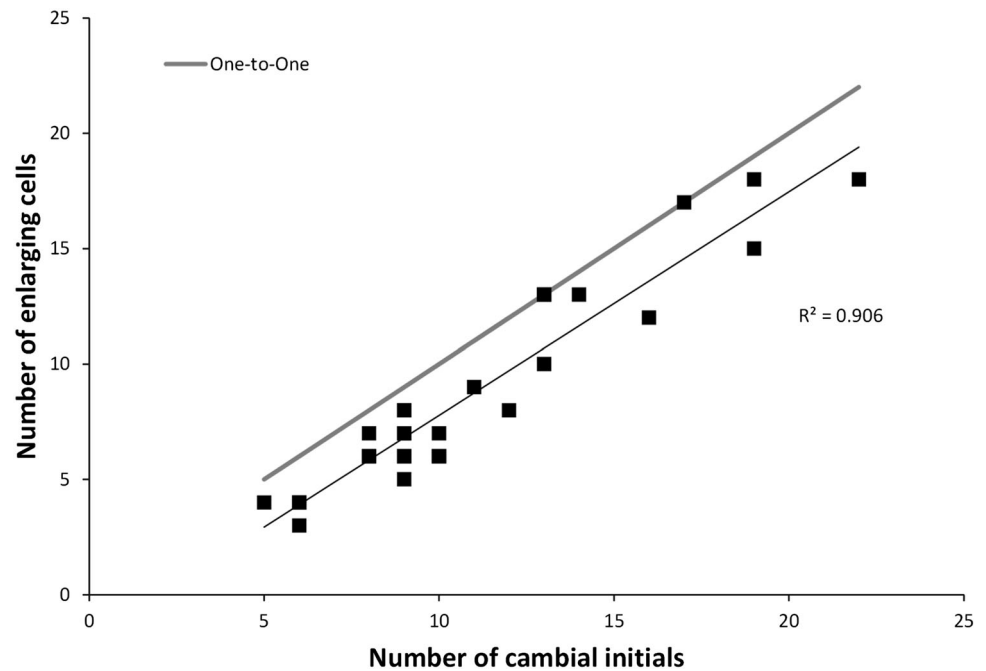


small adjustments, modeling phloem formation is also possible. In the xylem, cells move through three phases: division, enlargement and secondary thickening.

The tree will aim to maintain turgor in the developing cell population (see above) by modulating the size of the cambial and enlarging zones, while keeping the ratio of cambial to enlarging zones constant during the peak growing period. It has been shown in various studies that turgor is maintained at constant levels in cells in meristematic and expansion zones in plants (Nonami and Boyer 1989; Winship et al. 2010) and a constant ratio of cambial to enlarging cells, particularly during the early period of the growing season, is consistent with findings in various other species (Abe and Nakai 1999; Drew and Pammenter 2007; Drew et al. 2013; Rossi et al. 2006b, 2009; Shepherd 1964; Skene 1972) and in radiata pine for this study (Fig. 1).

For each daily time step, a cell $c$ will exit the cambial zone and enter the enlarging zone when:

- The ratio of enlarging to dividing cells exceeds a critical value adjusted as a function of the distance from the active buds (see Anfodillo et al. 2012; Ridoutt and Sands 1993, 1994) (Eq. 8).
- A meristematic cell does not exist between cell $c$ and the enlarging zone and

$$\alpha_{EZ/CZ} = \alpha_{EZ/CZ_{max}} \times \left(h_{tree} - h_{modpos}\right)\big/f_{juv}. \quad (8)$$

where $h_{tree}$ is the height of tree (m) and $h_{modpos}$ is the position on the stem at which the model is operating (m) on day and $\alpha_{EZ/CZ_{max}}$ and $f_{juv}$ are parameters.

Subsequently, after it has exited the cambial zone, a cell $c$ will exit the enlarging zone and enter the secondary thickening zone if:

- A growing cell does not exist between cell $c$ and the secondary thickening zone and
- The average osmotic potential in the dividing and enlarging cells zone exceeds $\Psi_{\pi_{crit}}$ and
- The number of growing days is greater than or equal to a critical minimum growing period (set here at 2 days).

Finally, cell $c$ will exit the secondary thickening zone and cease to differentiate if:

- A secondary thickening cell does not exist between cell $c$ and the functioning xylem and
- A maximum proportion of wall is reached (a parameter, $\alpha_{wall_{max}}$) or
- The cumulative carbohydrate concentration is below a threshold ($\gamma_{SUC_{CD}}$), or essentially when all carbohydrate has been used up.

At this point, the cell has undergone apoptosis, lost its protoplasm, and become a conductive element.

### Tracheid expansion

Cells in the dividing zone as well as the "true" enlargement zone undergo radial and longitudinal expansion. The rate of tracheid expansion is a process which is predominantly driven by turgor, and adjusted by the extensibility of the cell wall and the yield threshold (Abe and Nakai 1999; Cosgrove 2001; Hölttä et al. 2010; Kutschera 2004).

While a cell is in the phase of enlargement, the primary wall nominal thickness remains constant at 0.2 μm (Wardrop and Harada 1965). Radial wall extensibility (μm/MPa/day) in the process is predominantly modified by interactions with neighbours (i.e. a physical impedance which becomes greater as cells become larger and fill the available space) and drought severity (assuming that wall extensibility is an additional control of turgor) (Bogoslavsky and Neumann 1998; Cosgrove 2005) (Eq. 9).

$$\theta_c = \theta_{max} \times \left(1 - \left[\emptyset_c / \emptyset_{max}\right]\right) \times {}^{\Psi_{\pi_{crit}}}/\Psi_{\pi_{min}} \tag{9}$$

where $\emptyset_c$ is the radial diameter of cell $c$ (μm), $\Psi_{\pi_{crit}}$ is the critical osmotic potential on day (MPa), and $\theta_{max}$, $\emptyset_{max}$ and $\Psi_{\pi_{min}}$ are parameters.

In addition to extensibility control, the development of turgor (MPa) is osmotically adjusted (i.e. by the adjustment of solute concentration and osmotic potential in the vacuole) (Eq. 10).

$$\Psi_{p_c} = \min \begin{cases} \Psi_{p_{crit}} \\ \Psi_{xylem} - \Psi_{\pi_c} \end{cases} \tag{10}$$

where $\Psi_{xylem}$ is the mean water potential in the xylem at the modeled stem position (MPa) on day, $\Psi_{\pi_c}$, the osmotic potential of cell c (MPa), is defined above and $\varphi_{p_{crit}}$ is a parameter.

Total daily radial growth (μm/day) in cell $c$ for day is then calculated according to Eq. 11:

$$\Delta\emptyset_c = \theta_c \times \left(\Psi_{p_c} - \Psi_{p_{YT}}\right) \tag{11}$$

where $\theta_c$ is the wall extensibility of cell $c$ (Eq. 9) on day, $\Psi_{p_c}$ is the turgor pressure of cell $c$ (Eq. 10) and $\Psi_{p_{YT}}$ is a parameter.

Growth in the length of the tracheid (μm/day) is modelled as proportional to the radial growth (Eq. 12). This approach is very simple, and is an area where further research and development would be of particular value.

$$\Delta L_c = \min \begin{cases} \Delta\emptyset_c \times \propto_{\Delta\emptyset L} \\ L_{max} \end{cases} \tag{12}$$

where $\Delta\emptyset_c$ is the radial growth rate of cell $c$ on day (μm/day) (Eq. 11) and $\propto_{\Delta\emptyset L}$ and $L_{max}$ are parameters.

## Cell division

If cells are in the cambial zone, they will have the potential to divide. However, for each daily time step, a cell $c$ will only divide if:

- The radial diameter of cell $c$ exceeds a minimum value (Hölttä et al. 2010).
- The time since a previous mitosis in cell $c$ exceeds a minimum duration ($t_{div_{min}}$, a parameter) (Hölttä et al. 2010; Larson 1969).

- The amount of non-structural carbohydrate accumulated in the cell exceeds the amount required to build a new cell plate and a nominal quantity of new cellular organelles and other protoplasmic material.

Each daughter cell has a radial diameter equal to half the diameter of the mother cell. However, the option exists to randomize the diameter of the two cells resulting from a division by between 40 and 60 %. Because anticlinal divisions are not explicitly modeled, the length of the daughter cell, as well as the mother cell, following each periclinal division is reduced as would be expected if the division was pseudo-transverse. The daughter cell is the cell which arises on the pith-side of the original mother cell, following a division.

## Tracheid secondary thickening

Secondary wall formation utilizes carbohydrate accumulated in the cell during the stages of division and growth, as well as any carbohydrate that is subsequently allocated to the cell directly during the secondary thickening phase. Once secondary thickening commences, the rate of change of wall volume for cell $c$, on day, is calculated (Eq. 13).

$$\Delta V_{wall_c} = \min \begin{cases} \Delta V_{wall_{max}} \\ SUC_c \times \left({}^1/\rho_{CW}\right) \times 10^{12} \end{cases} \tag{13}$$

where $SUC_c$ is the accumulated quantity of carbohydrate (g) in cell $c$ on day and $\Delta V_{wall_{max}}$ and $\rho_{CW}$ are parameters.

The lumen volume (μm³) of cell $c$ is then re-calculated (Eq. 14).

$$V_{lum_c} = \max \begin{cases} (1 - \alpha_{wall_{max}}) \times V_c \\ V_{lum_c} - \Delta V_{wall_c} \end{cases} \tag{14}$$

where $V_c$ is the total volume of cell $c$ (μm³), $V_{lum_c}$ is the lumen volume of cell $c$ (μm³), $\Delta V_{wall_c}$ is the change in wall volume in cell $c$ on day (Eq. 13) and $\alpha_{wall_{max}}$ is a parameter.

If wall volume is greater than $\alpha_{wall_{max}} \times V_c$ (where $V_c$ is the volume of cell $c$) then the cell has reached the maximum possible wall thickness, and exits the phase of secondary thickening. Potential cell lumen surface area of cell $c$ (μm²) (supposing that the cell is a long, narrow rectangular prism) is calculated as (Eq. 15):

$$SA_{lum_c} = V_{lum_c}/L_c \tag{15}$$

where $V_{lum_c}$ is the lumen volume of cell c (μm³) (Eq. 14) and $L_c$ is the length of cell $c$ (μm) on day.

Wall thickness (μm) is finally determined using an optimization routine that calculates the wall thickness corresponding to a cell with known tangential and radial diameter with the calculated lumen surface area.

## Microfibril angle

The mechanism of microfibril angle orientation is still very poorly understood, particularly in woody perennials (Auty et al. 2013; Barnett and Bonham 2004; Donaldson 2008). To our knowledge, no model of MFA adjustment, in the context of broader framework around cambial activity and whole–tree physiology, currently exists. MFA has been linked, however, to rates of growth and subsequent wall development (Chan 2011; Donaldson 2008) and marked growth responses after releases from drought (Wimmer et al. 2002). In addition, findings in model species like *Arabidopsis* suggest that Cellulose Synthase A (CesA) activity as well as cellulose deficiencies can disturb microtubule orientation (Panteris et al. 2013). Microtubules are thought to be a key part of microfibril orientation (Chan 2011; Lloyd 2006). If so, cellulose availability and incorporation into the cell wall may be expected to impact on microfibril angle. Thus microfibril angle, given established links with growth rate, is calculated in the model using a calibrated function of the distribution of carbohydrate ($\alpha_{alloc}$) across the varying cambial and enlarging zones, and adjusted from tree age (Eq. 16). Microfibril angle is further adjusted according to predicted stem slenderness as MFA has been shown to be negatively correlated with height/diameter ratio in *P. radiata* (Lasserre et al. 2009). Associated with mechanical optimization of stem stiffness (Lachenbruch et al. 2011), the sensitivity of MFA is adjusted depending on the height and diameter of the tree (Eq. 16).

$$\text{MFA}_c = \text{MFA}_{max} \times \left( \alpha_{alloc}^{f_{MFA} \times SR} \right) \times \left( \#\text{rings}_p / 40 \right)^2 \quad (16)$$

where $\alpha_{alloc}$ is the allocation coefficient on day (see section above), SR is the slenderness ratio of the tree [in this case, stem diameter at the modeled position (cm)/height above modeled position(m)] and $\#\text{rings}_p$ is the ring count at position $p$ on day and $\text{MFA}_{max}$ and $f_{MFA}$ are parameters.

## Results and model performance

Outputs from the CaBala model, upon which wood property predictions were based, predicted 90 % of the variation in tree overbark diameter at breast height (DBH) (Fig. 2).

### Model outputs

#### Wood density

Predicted data explained about 80 % of the variation in average pith-to-bark wood density from 17 sites (Fig. 3). Average wood density in the outer 50 mm was not predicted as strongly ($R^2 = 0.77$), but still better than
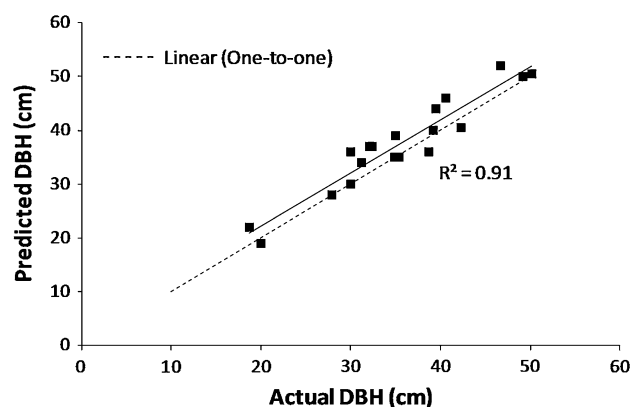


**Fig. 2** Tree diameter at breast height (DBH) predicted by the Cabala model vs. actual measured DBH, with the corresponding one-to-one relationship indicated by the *dotted line*

predictions in the juvenile core (first 10 rings) ($R^2 = 0.52$). Overall, there was a tendency for under-prediction of outerwood density at those sites with the highest average wood density. The inner core prediction was reduced most markedly by over-prediction in juvenile wood density at three sites (Figs. 4, 5).

### MFA

The model predictions of MFA were weaker than for density, with the model explaining 40 % and 50 % of the variation in average and outer core MFA respectively (Fig. 3). Model predictions of juvenile core MFA were not significantly correlated with measured values ($P = 0.07$). Overall, the correlation between modelled vs. measured MFA was significant ($P < 0.001$), but this was driven by two high MFA sites in New Zealand. The correlation was reduced by the over-prediction of MFA in two treatments at the Mt Gambier site and under-prediction of MFA at the Longford site (Fig. 6).

### Prediction of trends

The model predictions of tracheid radial diameter and wall thickness matched measured data (which was only available at 6 sites) reasonably well (Fig. 4). The model captured the increase in radial diameter in the first few rings at most sites. At the unthinned Flynn site, the model under-predicted mean ring tracheid radial diameter as the trees experienced putatively high levels of drought in the last 10 years of the simulation. This was linked to excessively reduced widths of the simulated enlarging zone, and concomitantly, reduced enlargement durations (data not shown). Wall thickness predictions were close to the measured values however. At the Ohurakura site, although tracheid radial diameter was predicted reasonably well, average ring wall thickness was

**Fig. 3** Model predicted vs. measured **a** wood density, **b** modulus of elasticity (MOE) and **c** microfibril angle (MFA) for 20 scenarios. Data are for a whole "core", average of the outer 50 mm and for the average of the first 10 annual rings (the juvenile core). *Solid lines* show regression on average core data; *dotted blue lines* show regression on outerwood data; *dotted grey lines* show the one-to-one line for the variable (colour figure online)
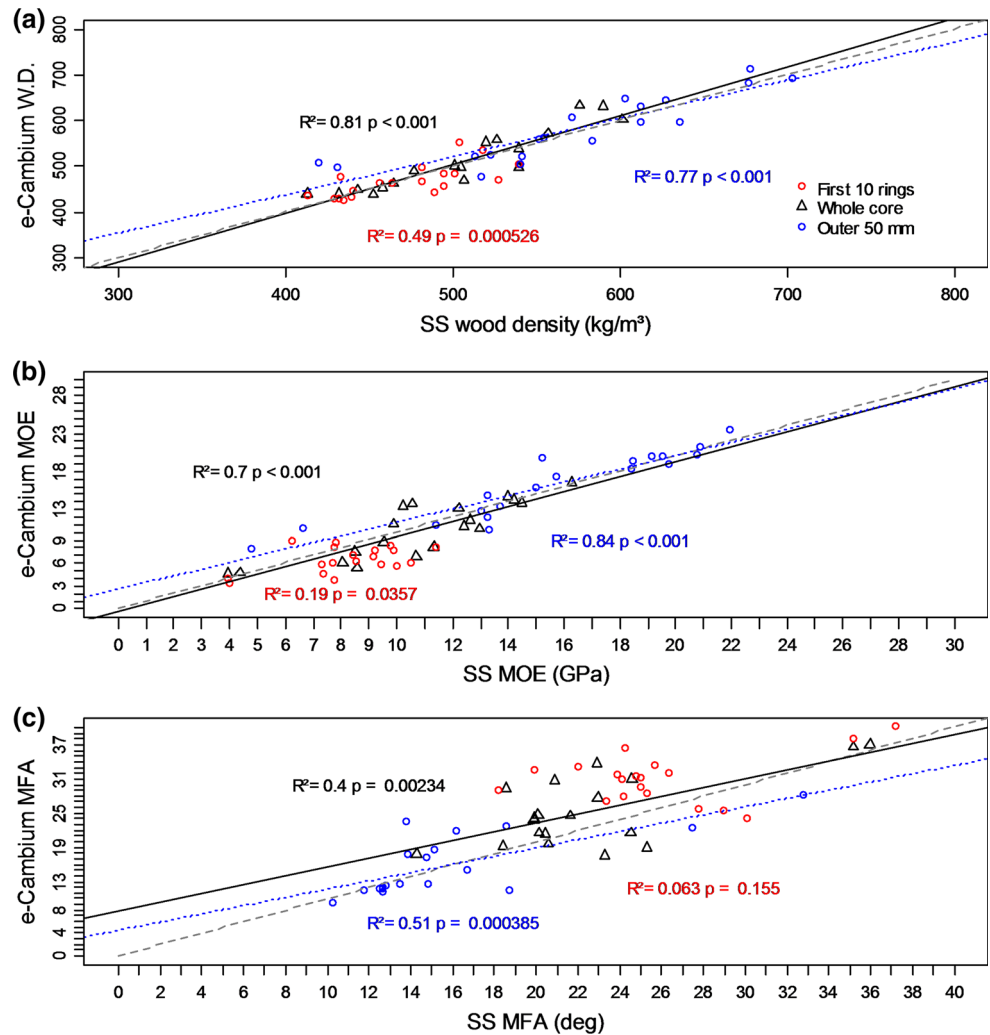


consistently over-predicted in the last 10 years of the simulation. At Balmoral, wall thickness was over-predicted in the final years of the simulation and tracheid diameter was over-predicted in the juvenile core.

The model predicted pith-to-bark trends in wood density well at most sites (Fig. 5). Wood density in the outer rings was over-predicted at the very low density New Zealand sites, due to the over-prediction of wall thickness in those cases. Wood density at the oldest stand (Caroline), McGillivrays and Byjuke (all characterised by high average wood density) was over-predicted in the early years, but accurately captured later. Note that unusually high predictions or data at the end or beginning of series is related to calculations being performed on partial rings.

Despite the poor correlations between predicted and actual average MFA, the model did capture the pith-to-bark trends in MFA well at most sites (Fig. 6). At the Mt Gambier site, the relatively sudden decline in MFA in the first few years was not captured. At Longford, although the pattern of pith-to-bark variation was reasonably accurate,

the model consistently under-predicted MFA. The sudden increase in MFA following severe thinning at the Flynn site was well captured by model predictions.

## Prediction of intra-annual patterns of wood variation

The model accurately captured the intra-annual pattern of wood density variation (Fig. 7). There was, however, a tendency for the predicted wood density to be higher in the latewood than was actually measured in outer rings, but this was associated with large error, mainly because only a small number of sites actually reached ages >30 years.

The model captured the intra-ring variation tracheid radial diameter and wall thickness reasonably well at the five sites from which complete (or nearly complete) pith-to-bark data was available (Fig. 8). Earlywood tracheid radial diameter was under-predicted and latewood radial diameter was over-predicted. The modelled data showed a slower decline in radial diameter from earlywood to

**Fig. 4** Trajectories of modelled annual (ring) mean tracheid radial diameter (*black circles*) and wall thickness (*grey crosses*) shown with minimum and maximum values of measured data (*blue lines*). Measured data were only available at some sites (colour figure online)
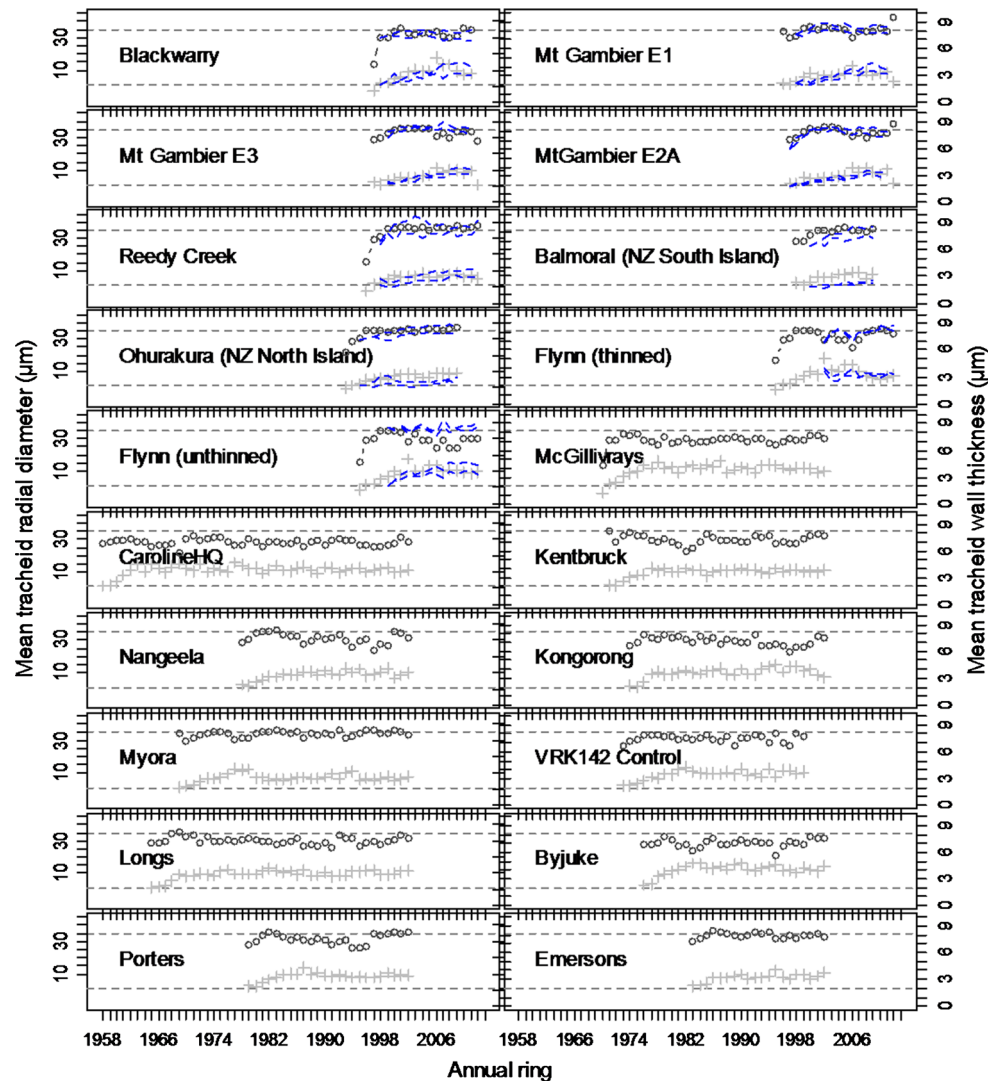


latewood than was observed in the actual data. The predicted patterns varied widely between modelled scenarios, however.

## Discussion

We have presented a model of fine-scale variation in wood formation and stem growth processes that essentially utilises only two elements: the carbon allocation balance and tree water status. Based on this parsimonious approach, the model did indeed significantly explain variation across 17 diverse stands of plantation-grown *P. radiata*, constrained across the full range by a single set of parameters. We recognise, however, that other factors still influence wood formation processes in ways which the model is not capturing, and further work is needed. The model represents, in our view, a framework for thinking about the basic

elements of wood formation from which further research and model concepts can easily be developed.

There can be no doubt that in reality, the causes of variation in wood properties are complex, as xylem differentiation can take place over several weeks, or even months, and is influenced by constantly changing conditions in the whole tree (Denne and Dodd 1981; Larson 1994).

### Model skill

The accuracy of model predictions of wood density is promising, with model outputs explaining 80 % of the variation measured on pith-to-bark core samples from 17 varied stands of *P. radiata*, each grown under quite different conditions and silvicultural regimes. The model predictions of averages and trends were also generally good. This is particularly encouraging because the quality
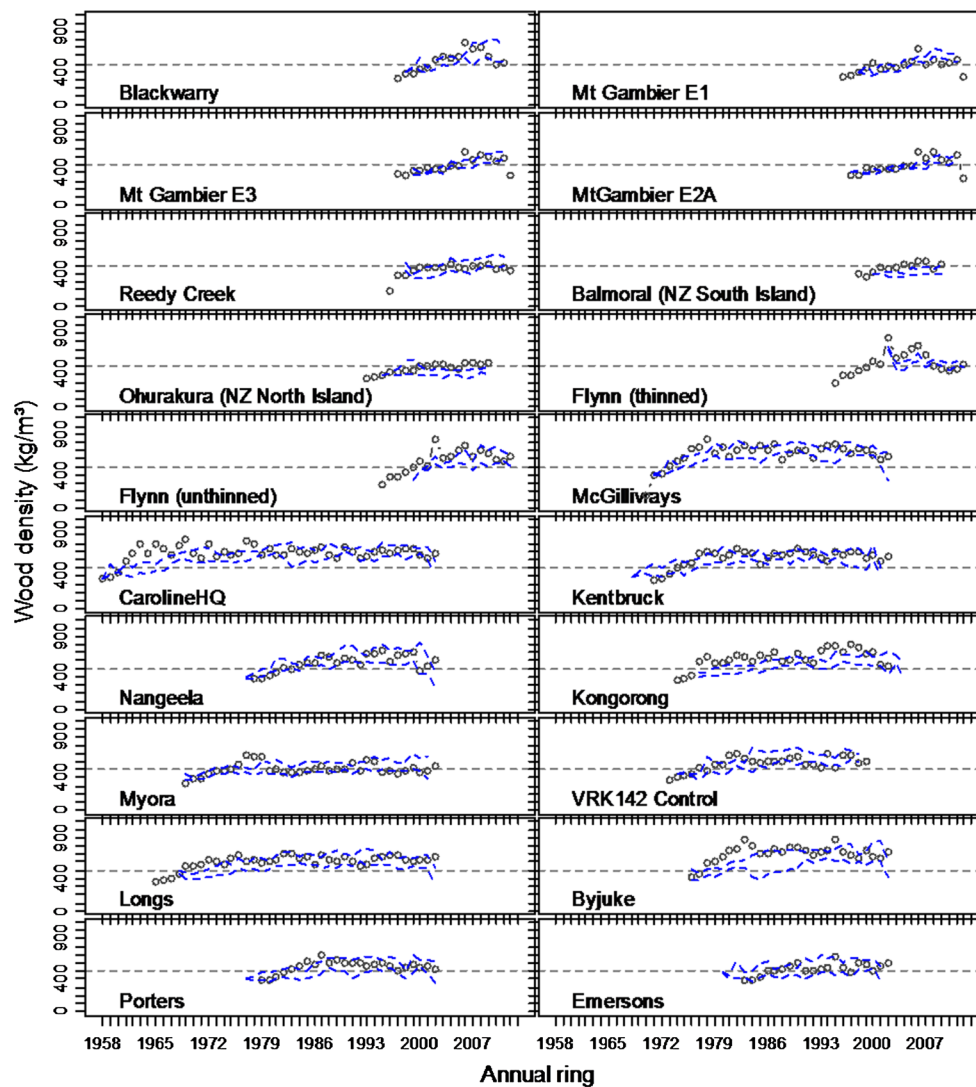
**Fig. 5** Trajectories of modelled annual (ring) mean wood density (*black circles*) for 20 modelled scenarios shown with minimum and maximum values of measured data (*blue lines*) (colour figure online)

of data available for site and regime was variable, and we were unable to be sure in some cases how accurately we had characterised growing conditions. Overall, the model correctly captured the pith-to-bark, as well as intra-annual, patterns and tendencies in tracheid radial diameter, tracheid wall thickness and wood density and MFA (see Burdon et al. 2004). The patterns at both scales are not constant between different stands of trees, and the model was able to handle variations in the general tendency, depending on effects of site or silviculture or weather. This is one of the strengths of an approach that incorporates aspects of the wood formation process. We believe that a particularly novel aspect of the model is the attempt to model pith-to-bark MFA variation as a function of cambial vigour and drought limitation. To our knowledge, our attempt to incorporate a relatively high-level model of

microfibril orientation in a broader framework is the first of its kind.

In cases where predictions of wood density did not match actual data, it was not always possible to determine specifically the cause of the discrepancy. Given the hierarchical data flow (i.e., using inputs from a pre-existing simulation) it was generally not possible to know to what extent input stand level data were inaccurate. Detailed data on actual leaf water potential, carbon fixation and allocation, and even metrics like leaf area index are typically scarce, covering only brief periods of time (the case in our study). Thus it was only possible to assess Cabala outputs on relatively easily measurable metrics such as DBH, for which reliable data was generally available. Furthermore, errors in silvicultural information (e.g. timing or intensities of thinning) or site descriptions would have a marked effect

**Fig. 6** Trajectories of modelled annual (ring) mean MFA (*black circles*) for 20 modelled scenarios shown with minimum and maximum values of measured data (*blue lines*) (colour figure online)
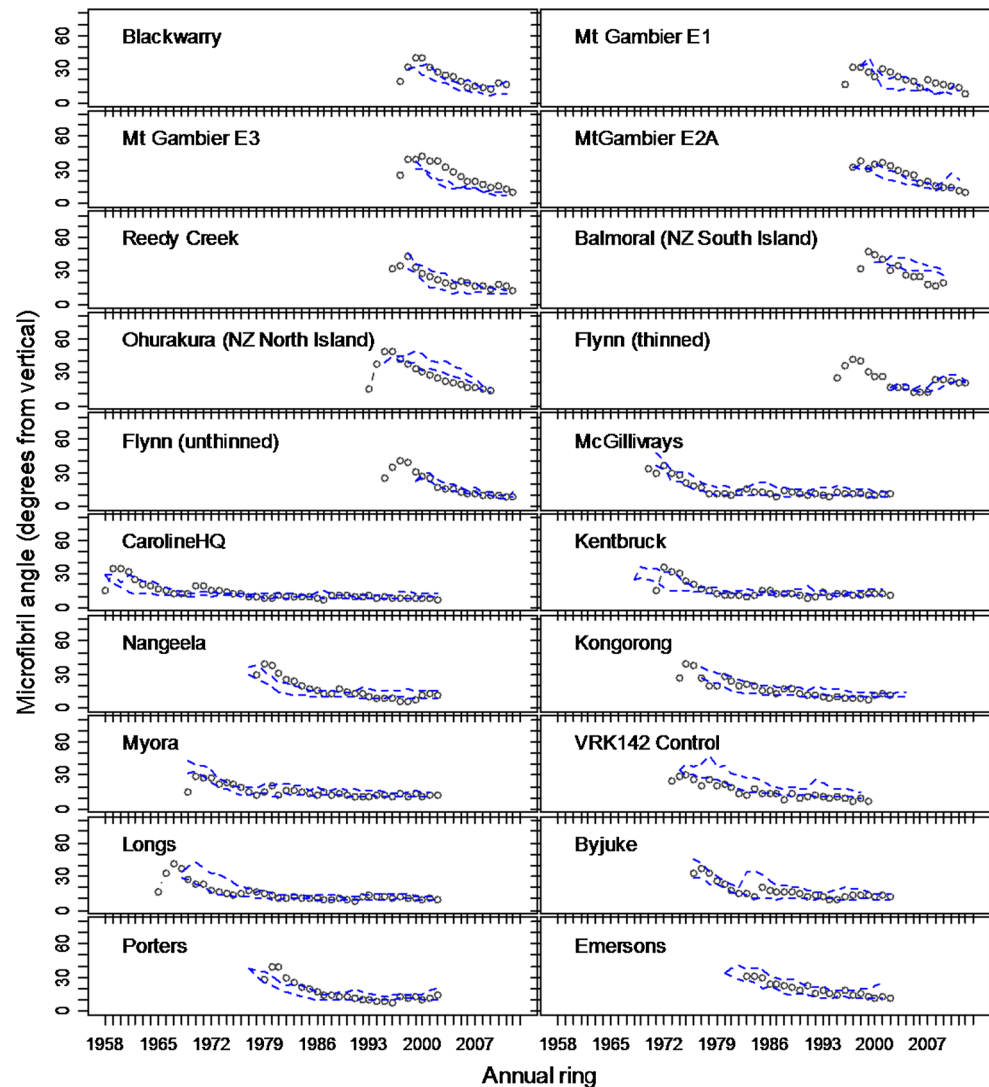


on predicted values. These data were not always known for the sites used in our study, and certain estimates had to be made based on general forestry practices or relatively coarse-scaled soil information. Another issue arises from wood quality variability not accounted for in the modelling framework, most notably, compression wood. It is likely that some reaction wood would have been present in many samples, which would have introduced uncontrolled variation. Another important element that is not directly taken into account in this model is the effect of nitrogen fertility on early-wood proportion. Although at our study sites we believe this effect was not of great importance, in cases where forests are established on highly nitrogen fertile ex-pasture sites, further model development may be required.

Overall we identified that model performance was weak in three areas. First, the model tended to under-predict tracheid radial diameter under conditions of relatively severe drought (particularly competition-induced instances,

such as in the case of the Flynn site). To what extent the simulated input values were realistic is not clear. Assuming they were accurate, however, it was evident that the model tended to excessively reduce enlargement duration. However, the control of turgor could also be improved in regard to tracheid expansion, and more explicit consideration of the role of other substances in the process, e.g. potassium (Fromm 2013), could potentially lead to some improvement in the predictions.

Second, the model over-predicted wall thickness in the latewood at some sites, mainly due to overly strong flow of carbohydrates as the cambial zone constricted. This problem may be due in part to errors in the predicted timing of allocation and carbohydrate flows in the whole tree, as well as to problems with the embedded concepts of latewood formation and control itself. In dealing with this issue, further research is needed around the determination of the onset of programmed cell death. This is currently
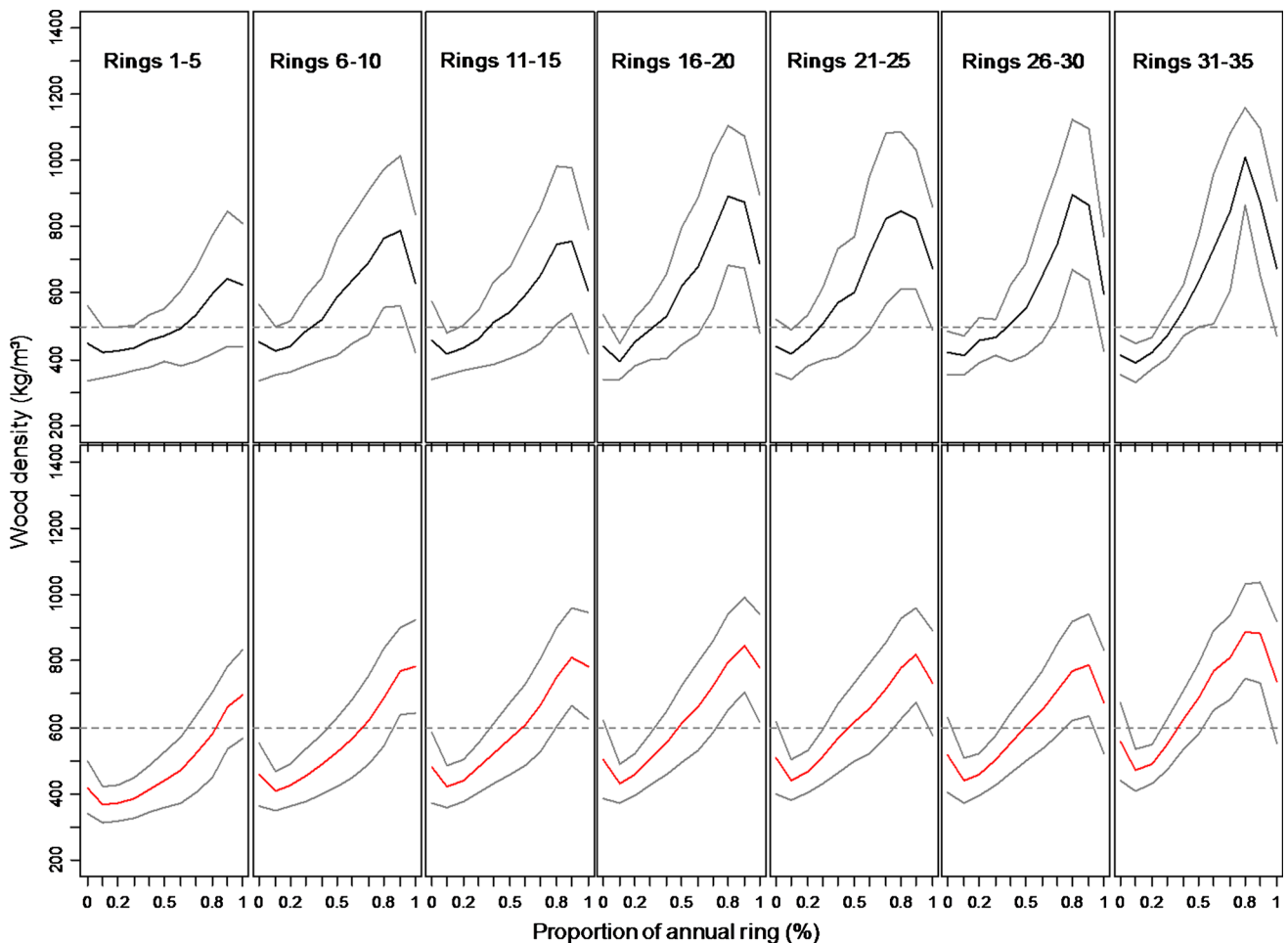
**Fig. 7** Simulated (*black lines*; lower graphs) and actual (*red lines*; lower graphs) intra-annual patterns of wood density variation across a normalised annual ring. *Grey lines* show mean ± standard deviation (for the 5-ring means). *Grey lines* show mean ± 1 standard deviation (colour figure online)

controlled by the reduction in sucrose concentration in the cell (Bollhöner et al. 2012). It is also possible that secondary wall thickening may be tied to the accumulation of localised serine proteases, regulated in turn by the expression of protease inhibitor genes (Escamez and Tuominen 2014). Some initial tests of an implementation of this idea in the model were promising, yielding similar results to the approach based on sucrose concentrations (data not shown).

Third, predictions were consistently weakest in the juvenile core (the first 10 rings). It is important, in elucidating this issue, to recognise the greater uncertainty associated with wood property measurements close to the pith. Few trees are perfectly round, and often trees have eccentric piths, or cored samples do not follow the radius, which means that the first few rings cannot be measured as accurately as outer rings, even though SilviScan is capable of limited sample re-orientation. Nevertheless, this is only part of the puzzle. As understanding juvenile wood quality is of key importance to forest management as rotation

lengths decrease, further work is needed. In the model, control of juvenile wood formation processes is adjusted as an elementary function of distance from live-crown. How this effect actually occurs, however, is undoubtedly highly complex, involving interactions between multiple factors, including several hormones, gene expression controls and carbohydrate gradients (Li et al. 2012; Paulina Fernández et al. 2007; Plomion et al. 2001). Although it has been our goal to keep the model as parsimonious as possible, in order to address some of these model weaknesses, it may be necessary to increase the sophistication of some modules.

## The usefulness of this modelling approach for commercial applications

So-called process-based models of forest growth have improved considerably in recent years, to the point where they have become useful management tools (Almeida et al. 2004; Battaglia and Sands 1997; Landsberg and Sands 2010;
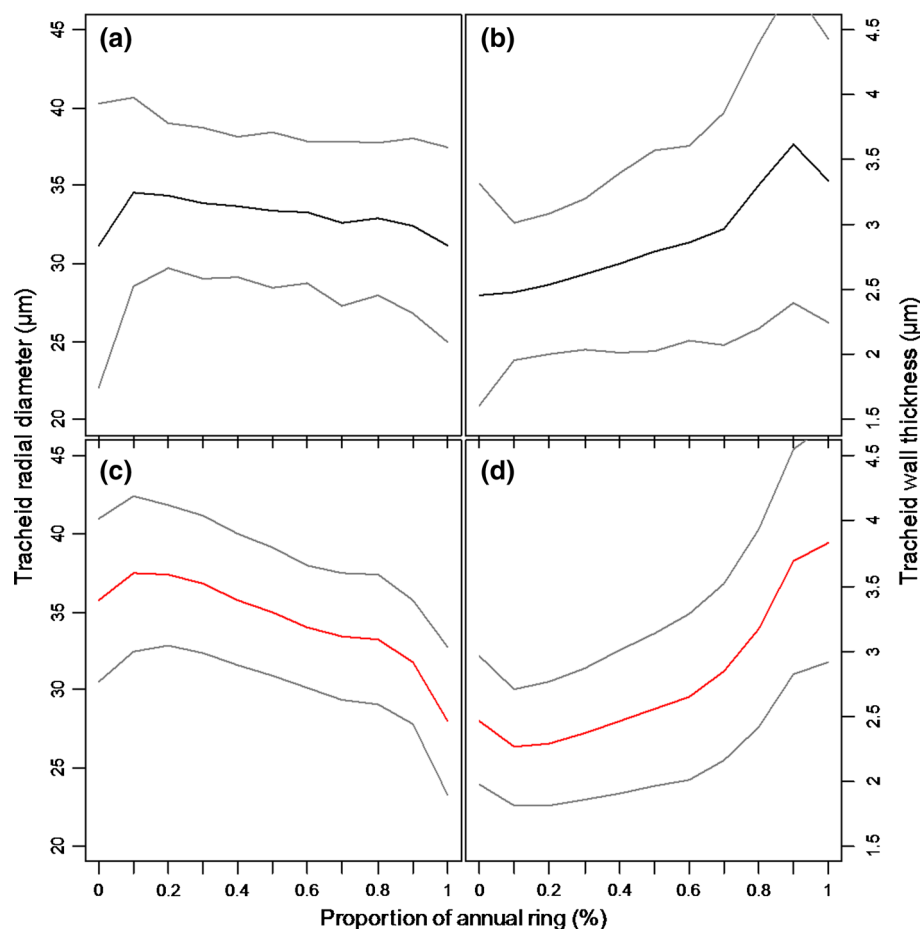
Sands [2004]). The value of this approach is that it theoretically makes scenario exploration possible beyond the bounds of existing data and field experience. That is, stand growth responses and tree performance can be forecast under hypothetical future conditions for which there may be little if any precedent (e.g. increasing average temperatures, changing rainfall patterns or a new silvicultural intervention). Inasmuch as it is valuable to understand how tree growth may vary (i.e. how big trees will get, or volume of wood expected from a stand), it is also of importance to understand what changing conditions or management might do to wood quality.

A model framework as we have described makes it possible to explore the potential result of leaving an existing site to grow for an extended period into the future, using modelled climate data. Given increasing levels of uncertainty around future climate variability, models of wood formation are potentially very useful for understanding future risks in managed forests, both in terms of productivity and wood quality (cf. Pinkard and Bruce [2011]). Forest growers can also explore the potential wood quality implications of alternative management regimes (e.g. changing the timing of thinning events). We believe that the model presented here provides a testable means of exploring our understanding of several aspects of

xylogenesis, and highlighting areas where further research may be needed.

# References

Abe H, Nakai T (1999) Effect of the water status within a tree on tracheid morphogenesis in *Cryptomeria japonica*. Trees 14:124–129

Almeida AC, Landsberg JJ, Sands PJ, Ambrogi MS, Fonseca S, Barddal SM, Bertolucci FL (2004) Needs and opportunities for using a process-based productivity model as a practical tool in *Eucalyptus* plantations. For Ecol Manag 193:167–177

Anfodillo T, Deslauriers A, Menardi R, Tedoldi L, Petit G, Rossi S (2012) Widening of xylem conduits in a conifer tree depends on the longer time of cell expansion downwards along the stem. J Exp Bot 63:837–845

Apiolaza L, Chauhan S, Hayes M, Nakada R, Sharma M, Walker J (2013) Selection and breeding for wood quality A new approach. N Z J For 58:32–37

Auty D, Gardiner B, Achim A, Moore J, Cameron A (2013) Models for predicting microfibril angle variation in Scots pine. Ann For Sci 70:209–218

Barnett JR (1973) Seasonal Variation in the ultrastructure of the cambium in New Zealand grown *Pinus radiata* D. Don. Ann Bot Lond 37:1005–1011

Barnett JR, Bonham VA (2004) Cellulose microfibril angle in the cell wall of wood fibres. Biol Rev 79:461–472

Battaglia M, Sands P (1997) Modelling site productivity of *Eucalyptus globulus* in response to climatic and site factors. Aust J Plant Physiol 24:831–850

Battaglia M, Sands P, White D, Mummery D (2004) CABALA: a linked carbon, water and nitrogen model of forest growth for silvicultural decision support. For Ecol Manag 193:251–282

Bauerle WL, Oren R, Way DA, Qian SS, Stoy PC, Thornton PE, Bowden JD, Hoffman FM, Reynolds RF (2012) Photoperiodic regulation of the seasonal pattern of photosynthetic capacity and the implications for carbon cycling. Proc Natl Acad Sci 109:8612–8617

Boardman R (1988) Living on the edge—the development of silviculture in South Australian pine plantations. Aust For 51:135–156

Bogoslavsky L, Neumann PM (1998) Rapid regulation by acid pH of cell wall adjustment and leaf growth in Maize plants responding to reversal of water stress. Plant Physiol 118:701–709

Bollhöner B, Prestele J, Tuominen H (2012) Xylem cell death: emerging understanding of regulation and function. J Exp Bot 63:1081–1094

Burdon RD, Kibblewhite RP, Walker JC, Megraw RA, Evans R, Cown DJ (2004) Juvenile versus mature wood: a new concept, orthogonal to corewood versus outerwood, with special reference to *Pinus radiata* and *P. taeda*. For Sci 50:399–415

Catesson AM, Roland JC (1981) Sequential changes associated with cell wall formation and fusion in the vascular cambium. IAWA Bull 2:151–162

Chan J (2012) Microtubule and cellulose microfibril orientation during plant cell and organ growth. J Microsc 247(1):23–32

Cosgrove DJ (2001) Wall structure and wall loosening. A look backwards and forwards. Plant Physiol 125:131–134

Cosgrove DJ (2005) Growth of the plant cell wall. Nat Rev Mol Cell Biol 6:850–861

Deckmyn G, Evans SP, Randle TJ (2006) Refined pipe theory for mechanistic modelling of wood development. Tree Physiol 26:703–717

Deleuze C, Houllier F (1998) A simple process-based xylem growth model for describing wood microdensitometric profiles. J Theor Biol 193:99–113

Denne MP (1971) Temperature and tracheid development in *Pinus sylvestris* seedlings. J Exp Bot 22:362–370

Denne MP (1976) Effects of environmental change on wood production and wood structure in *Picea sitchensis* seedlings. Ann Bot Lond 40:1017–1028

Denne MP, Dodd RS (1981) The environmental control of xylem differentiation. In: Barnett JR (ed) Xylem cell developement. Castle House Publications, Kent, pp 236–255

Dodd RS, Fox P (1990) Kinetics of tracheid differentiation in Douglas-fir. Ann Bot Lond 65:649–657

Donaldson L (2008) Microfibril angle: measurement, variation and relationships—a review. IAWA J 29:345–386

Downes GM, Drew DM (2008) Climate and growth influences on wood formation and utilisation. South For 70:155–167

Downes GM, Beadle C, Gensler W, Mummery D, Worledge D (1999) Diurnal variation and radial growth of stems in young plantation eucalypts. In: Wimmer R, Vetter RE (eds) Tree ring analysis. Biological, methodological and environmental aspects. CAB International, New York, pp 83–104

Downes GM, Wimmer R, Evans R (2004) Interpreting sub-annual wood property variation in terms of stem growth. Wood fibre cell walls: methods to study their formation, structure and properties. Swedish University of Agricultural Sciences, Department of Wood Science, pp 267–283

Drew DM, Pammenter NW (2007) Developmental rates and morphological properties of fibres in two eucalypt clones at sites differing in water availability. South Hemisph For J 69:71–79

Drew DM, Downes GM, Battaglia M (2010) CAMBIUM, a process-based model of daily xylem development in *Eucalyptus*. J Theor Biol 264:395–406

Drew DM, Richards AE, Cook GD, Downes GM, Gill W, Baker PJ (2013) The number of days on which increment occurs is the primary determinant of annual ring width in *Callitris intratropica*. Trees: 1–10

Duan H, Amthor JS, Duursma RA, O'Grady AP, Choat B, Tissue DT (2013) Carbon dynamics of eucalypt seedlings exposed to progressive drought in elevated [$CO_2$] and elevated temperature. Tree Physiol 65(5):1313–1321

Duchesne L, Houle D, D'Orangeville L (2012) Influence of climate on seasonal patterns of stem increment of balsam fir in a boreal forest of Québec. Canada Agric For Meteorol 162–163:108–114

Escamez S, Tuominen H (2014) Programmes of cell death and autolysis in tracheary elements: when a suicidal cell arranges its own corpse removal. J Exp Bot 65(5):1313–1321

Evans R (1994) Rapid measurement of the transverse dimensions of tracheids in radial wood sections from *Pinus radiata*. Holzforschung 48:168–172

Evans R, Ilic J (2001) Rapid prediction of wood stiffness from microfibril angle and density. For Prod J 51:53–57

Feikema PM, Morris JD, Beverly CR, Collopy JJ, Baker TG, Lane PNJ (2010) Validation of plantation transpiration in southeastern Australia estimated using the 3PG+ forest growth model. For Ecol Manage 260:663–678

Fernández MP, Norero A, Vera JR, Pérez E (2011) A functional–structural model for radiata pine (*Pinus radiata*) focusing on tree architecture and wood quality. Ann Bot Lond 108:1155–1178

Fritts HC (1976) Tree rings and climate. Academic Press, New York

Fritts HC, Shashkin A, Downes GM (1999) TreeRing 3: a simulation model of conifer ring growth and cell structure. In: Wimmer R, Vetter RE (eds) Tree ring analysis: biological, methodological and environmental aspects. CAB International, Oxford, pp 3–32

Fromm J (2013) Xylem development in trees: from cambial divisions to mature wood cells. In: Fromm J (ed) Cellular aspects of wood formation, vol 20. Springer, Berlin Heidelberg, pp 3–39

Gavran M, Parsons M (2011) Australian plantation statistics 2011. Australian Bureau of Agricultural and Resource Economics and Sciences, Canberra

Gričar J, Zupančič M, Čufar K, Oven P (2007) Regular cambial activity and xylem and phloem formation in locally heated and cooled stem portions of Norway spruce. Wood Sci Technol 41:463–475

Harashima H, Schnittger A (2010) The integration of cell division, growth and differentiation. Curr Opin Plant Biol 13:66–74

Haygreen JG, Bowyer JL (1982) Forest products and wood science: an introduction. Iowa State University Press, Ames, Iowa, p 495

Hölttä T, Mäkinen H, Nöjd P, Mäkelä A, Nikinmaa E (2010) A physiological model of softwood cambial growth. Tree Physiol 30:1235–1252

Horacek P, Slezingerova J, Gandelova L, Wimmer R, Vetter R (1999) Effects of environment on the xylogenesis of Norway spruce (Picea abies [L.] Karst.). In: Vetter RE (ed) Tree-ring analysis: biological, methodological and environmental aspects, pp 35–53

Kellogg RM, Wangaard FF (1969) Variation in the cell wall density of wood. Wood Fibre Sci 1:180–204

Kramer EM (2002) A mathematical model of pattern formation in the vascular cambium of trees. J Theor Biol 216:147–158

Kutschera U (2004) The biophysical basis of cell elongation and organ maturation in coleoptiles of rye seedlings: implications for shoot development. Plant Biol 6:158–164

Lachaud S (1989) Participation of auxin and abscisic acid in the regulation of seasonal variations in cambial activity and xylogenesis. Trees 3:125–137

Lachenbruch B, Moore J, Evans R (2011) Radial variation in wood structure and function in woody plants, and hypotheses for its occurrence. In: Meinzer FC, Lachenbruch B, Dawson TE (eds) Size- and age-related changes in tree structure and function, vol 4. Springer, Netherlands, pp 121–164

Landsberg JJ, Sands P (2010) Physiological ecology of forest production: principles, processes and models. Academic Press, London, p 352

Larson P (1969) Wood formation and the concept of wood quality. Yale University, New Haven, p 54

Larson P (1994) The vascular cambium: development and structure. Springer-Verlag, New York

Lasserre J-P, Mason EG, Watt MS, Moore JR (2009) Influence of initial planting spacing and genotype on microfibril angle, wood density, fibre properties and modulus of elasticity in Pinus radiata D. Don corewood. For Ecol Manag 258:1924–1931

Li X, Wu HX, Southerton SG (2012) Identification of putative candidate genes for juvenile wood density in Pinus radiata. Tree Physiol 32:1046–1057

Lloyd C (2006) Microtubules make tracks for cellulose. Science 312:1482–1483

Lupi C, Rossi S, Vieira J, Morin H, Deslauriers A (2014) Assessment of xylem phenology: a first attempt to verify its accuracy and precision. Tree Physiol 34:87–93

Meicenheimer RD, Larson P (1983) Empirical models for xylogenesis in Populus deltoides. Ann Bot Lond 51:491–502

Meinzer FC, Bond BJ, Karanian JA (2008) Biophysical constraints on leaf expansion in a tall conifer. Tree Physiol 28:197–206

Nonami H, Boyer JS (1989) Turgor and growth at low water potentials. Plant Physiol 89:798–804

Oda Y, Fukuda H (2012) Secondary cell wall patterning during xylem differentiation. Curr Opin Plant Biol 15:38–44

O'Hehir JF, Nambiar EKSN (2010) Productivity of three successive rotations of P. radiata plantations in South Australia over a century. For Ecol Manag 259:1857–1869

Panteris E, Adamakis I-DS, Daras G, Hatzopoulos P, Rigas S (2013) Differential responsiveness of cortical microtubule orientation to suppression of cell expansion among the developmental zones of Arabidopsis thaliana root apex. PLoS One 8:e82442

Paulina Fernández M, Norero A, Barthélémy D, Vera J (2007) Morphological trends in main stem of Pinus radiata D. Don: transition between vegetative and reproductive phase. Scand J For Res 22:398–406

Philipson WR, Ward JM, Butterfield BG (1971) The vascular cambium: its development and activity. Chapman and Hall, London

Pinkard EA, Bruce J (2011) Climate change and South Australia's plantations: impacts, risks and options for adaptation.

Department of Primary Industries of South Australia. http://pir.sa.gov.au/__data/assets/pdf_file/0011/233984/ForestrySA_impact_and_adaptation_report_FINAL_July_2011.pdf

Plomion C, Leprovost G, Stokes A (2001) Wood formation in trees. Plant Physiol 127:1513–1523

Ridoutt BG, Sands R (1993) Within-tree variation in cambial anatomy and xylem cell differentiation in Eucalyptus globulus. Trees 8:18–22

Ridoutt BG, Sands R (1994) Quantification of the processes of secondary xylem fibre development in Eucalyptus globulus at two height levels. IAWA J 15:417–424

Rossi S, Anfodillo T, Menardi R (2006a) Trephor: a new tool for sampling microcores from tree stems. IAWA J 27:89–97

Rossi S, Deslauriers A, Anfodillo T (2006b) Assessment of cambial activity and xylogenesis by microsampling tree species: an example at the alpine timberline. IAWA J 27:383–394

Rossi S, Deslauriers A, Anfodillo T, Morin H, Saracino A, Motta R, Borghetti M (2006c) Conifers in cold environments synchronize maximum growth rate of tree-ring formation with day length. New Phytol 170:301–310

Rossi S, Deslauriers A, Griçar J, Seo J-W, Rathgeber CBK, Anfodillo T, Morin H, Levanic T, Oven P, Jalkanen R (2008) Critical temperatures for xylogenesis in conifers of cold climates. Glob Ecol Biogeogr 17:696–707

Rossi S, Simard S, Rathgeber C, Deslauriers A, De Zan C (2009) Effects of a 20-day-long dry period on cambial and apical meristem growth in Abies balsamea seedlings. Trees Struct Funct 23:85–93

Sands PJ (2004) 3PGPJS vsn 2.4—a user-friendly interface to 3-PG, the Landsberg and Waring model of forest productivity. Cooperative Research Centre for Sustainable Production Forestry, Hobart

Sauter JJ (1980) Seasonal variation of sucrose content in the xylem sap of salix. Z für Pflanzenphysiol 98:377–391

Sauter JJ (2000) Photosynthate allocation to the vascular cambium: facts and problems. In: Savidge R, Barnett JR, Napier R (eds) Cell and molecular biology of wood formation. BIOS Scientific Publishers, Oxford, pp 71–83

Savidge RA, Wareing PF (1981) A tracheid-differentiation factor from pine needles. Planta 153:395–404

Shepherd KR (1964) Some observations on the effect of drought on the growth of Pinus radiata D. Don. Aust For 28:7–22

Skene DS (1969) The period of time taken by cambial derivatives to grow and differentiate into tracheids in Pinus radiata. Ann Bot Lond 33:253–262

Skene DS (1972) The kinetics of tracheid development in Tsuga canadensis and its relation to tree vigour. Ann Bot Lond 36:179–187

Steppe K, Lemeur R (2007) Effects of ring-porous and diffuse-porous stem wood anatomy on the hydraulic parameters used in a water flow and storage model. Tree Physiol 27:43–52

Uggla C, Magel E, Moritz T, Sundberg B (2001) Function and dynamics of auxin and carbohydrates during earlywood/latewood transition in scots pine. Plant Physiol 125:2029–2039

Vaganov EA, Hughes MK, Shashkin AV (2006) Growth dynamics of conifer tree rings: an image of past and future environments. Springer-Verlag, New York

Vavrčík H, Gryc V, Vichrová G (2013) Xylem formation in young Norway spruce trees in Drahany Highland, Czech Republic. IAWA J. 34:231–234

Walcroft AS, Silvester WB, Whitehead D, Kelliher FM (1997) Seasonal changes in stable carbon isotope ratios within annual rings of Pinus radiata reflect environmental regulation of growth processes. Funct Plant Biol 24:57–68

Wardrop AB (1981) Lignification and xylogenesis. In: Barnett JR (ed) Xylem cell development. Castle House Publications, Kent

Wardrop AB, Harada H (1965) The formation and structure of the cell wall in fibres and tracheids. J Exp Bot 16:356–371

Wilson BF (1964) A model of cell production by the cambium of conifers. In: Zimmerman MH (ed) The formation of wood in forest trees. Academic Press, New York, pp 19–36

Wilson BF, Howard RA (1968) A computer model for cambial activity. For Sci 14:77–90

Wimmer R, Downes GM, Evans R (2002) Temporal variation of microfibril angle in *Eucalyptus nitens* grown in different irrigation regimes. Tree Physiol 22:449–457

Winship LJ, Obermeyer G, Geitmann A, Hepler PK (2010) Under pressure, cell walls set the pace. Trends Plant Sci 15:363–369

Woodruff DR, Bond BJ, Meinzer FC (2004) Does turgor limit growth in tall trees? Plant Cell Environ 27:229–236

Wu HX, Ivković M, Gapare WJ, Baltunis BS, Powell MB, McRae TA (2008) Breeding for wood quality and profit in radiata pine: a review of genetic parameters. N Z J For Sci 38(1)

Zhang J, Nieminen K, Serra JAA, Helariutta Y (2014) The formation of wood and its control. Curr Opin Plant Biol 17:56–63

Zweifel R, Zimmerman L, Newbery DM (2005) Modeling tree water deficit from microclimate: an approach to quantifying drought stress. Tree Physiol 25:147–156

Zweifel R, Steppe K, Sterck FJ (2007) Stomatal regulation by microclimate and tree water relations: interpreting ecophysiological field data with a hydraulic plant model. J Exp Bot 58:2113–2131